





## RESEARCH ARTICLE

# Hyperosmolar expansion medium improves nucleus pulposus cell phenotype

Lisanne T. Laagland<sup>1</sup>  | Frances C. Bach<sup>1</sup> | Laura B. Creemers<sup>2</sup>  |  
Christine L. Le Maitre<sup>3</sup>  | Deepani W. Poramba-Liyanage<sup>1</sup> | Marianna A. Tryfonidou<sup>1</sup> 

<sup>1</sup>Department of Clinical Sciences, Faculty of Veterinary Medicine, Utrecht University, Utrecht, The Netherlands

<sup>2</sup>Department of Orthopedics, University Medical Centre Utrecht, Utrecht, The Netherlands

<sup>3</sup>Biomolecular Sciences Research Centre, Sheffield Hallam University, Sheffield, UK

## Correspondence

Marianna A. Tryfonidou and Deepani W. Poramba-Liyanage, Department of Clinical Sciences, Faculty of Veterinary Medicine, Utrecht University, Yalelaan 108, 3584 CM Utrecht, The Netherlands.

Email: [m.a.tryfonidou@uu.nl](mailto:m.a.tryfonidou@uu.nl) and [d.w.l.porambaliyanage@uu.nl](mailto:d.w.l.porambaliyanage@uu.nl)

## Funding information

Dutch Arthritis Society, Grant/Award Numbers: LLP12, LLP22; Horizon 2020 Framework Programme, Grant/Award Number: 825925

## Abstract

**Background:** Repopulating the degenerated intervertebral disc (IVD) with tissue-specific nucleus pulposus cells (NPCs) has already been shown to promote regeneration in various species. Yet the applicability of NPCs as cell-based therapy has been hampered by the low cell numbers that can be extracted from donor IVDs and their potentially limited regenerative capacity due to their degenerated phenotype. To optimize the expansion conditions, we investigated the effects of increasing culture medium osmolarity during expansion on the phenotype of dog NPCs and their ability to produce a healthy extracellular matrix (ECM) in a 3D culture model.

**Methods:** Dog NPCs were expanded in expansion medium with a standard osmolarity of 300 mOsm/L or adjusted to 400 or 500 mOsm/L in both normoxic and hypoxic conditions. Following expansion, NPCs were cultured in a 3D culture model in chondrogenic culture medium with a standard osmolarity. Read-out parameters included cell proliferation rate, morphology, phenotype and healthy ECM production.

**Results:** Increasing the expansion medium osmolarity from 300 to 500 mOsm/L resulted in NPCs with a more rounded morphology and a lower cell proliferation rate accompanied by the expression of several healthy NPC and progenitor markers at gene (*KRT18*, *ACAN*, *COL2*, *CD73*, *CD90*) and protein (*ACAN*, *PAX1*, *CD24*, *TEK*, *CD73*) level. The NPCs expanded at 500 mOsm/L were able to retain most of their phenotypic markers and produce healthy ECM during 3D culture independent of the oxygen level used during expansion.

**Conclusions:** Altogether, our findings show that increasing medium osmolarity during expansion results in an NPC population with improved phenotype, which could enhance the potential of cell-based therapies for IVD regeneration.

## KEYWORDS

cell-based therapy, intervertebral disc, lower back pain, nucleus pulposus, osmolarity, regeneration

**Abbreviations:** ECM, extracellular matrix; GAG, glycosaminoglycan; HX, hypoxia; IVD, intervertebral disc; LBP, lower back pain; MSC, mesenchymal stem cell; NC, notochordal cell; NP, nucleus pulposus; NPC, nucleus pulposus cell; NX, normoxia.

Deepani W. Poramba-Liyanage and Marianna A. Tryfonidou contributed equally to this study.

This is an open access article under the terms of the [Creative Commons Attribution-NonCommercial](https://creativecommons.org/licenses/by-nc/4.0/) License, which permits use, distribution and reproduction in any medium, provided the original work is properly cited and is not used for commercial purposes.

© 2022 The Authors. *JOR Spine* published by Wiley Periodicals LLC on behalf of Orthopaedic Research Society.

## 1 | INTRODUCTION

Lower back pain (LBP) is a major health and socioeconomic problem worldwide with more than 80% of the human population experiencing LBP at least once in their life.<sup>1,2</sup> Degeneration of the intervertebral disc (IVD) is a common cause of chronic LBP.<sup>3–5</sup> When IVD degeneration has progressed to a stage where pain and loss of function can no longer be managed by conservative means, surgery remains a last-resort treatment. Therefore, new innovative treatment strategies that promote regeneration of the mild to moderately degenerate IVD are urgently needed.

The IVD is the largest avascular organ in the body with a low partial pressure of oxygen ( $pO_2$ ) varying from 5% to 1%  $O_2$  in the core of the IVD, the nucleus pulposus (NP).<sup>6,7</sup> The extracellular matrix (ECM) of the healthy NP is highly hydrated and mainly composed of proteoglycans intermixed with collagen type II.<sup>8</sup> Cations, which are attracted to the negatively charged proteoglycans, create a strong osmotic gradient that draws water molecules into the healthy NP.<sup>8</sup> This osmotic gradient in a confined space, where tissue swelling is prevented, causes a high intradiscal pressure enabling the NP to function as a hydraulic cushion. It is in the NP that the first signs of tissue degeneration are encountered.<sup>9</sup> As the IVD degenerates, the NP glycosaminoglycan (GAG) content gradually decreases, which causes a drop in osmolarity, resulting in a decreased water content of the NP. Furthermore, the flexible collagen type II is replaced by the more rigid collagen type I.<sup>10</sup> As a result, the IVD fails to fulfill its biomechanical role and further deteriorates by subsequent physiological loading.<sup>11,12</sup>

Previous *in vivo* studies showed that the synthesis of healthy NP ECM can be stimulated by growth factors that are injected into the IVD and/or gene therapy.<sup>13,14</sup> However, stimulation of the remaining NP cell (NPC) population is often insufficient to achieve regeneration because of the loss of viable cells and the shift to a degenerated phenotype.<sup>8,15–17</sup> Therefore, repopulating the degenerated NP using cell-based therapies is considered a promising approach for biologically restoring the IVD. To date, several different cell sources are investigated for NP regeneration (reviewed in Williams et al.<sup>18</sup>). Clinical trials that have employed allogeneic mesenchymal stromal cells (MSCs) have reported clinical improvement in pain and function, but there is no clear evidence for regeneration of the diseased IVD.<sup>19,20</sup> MSCs have been shown to exert immunosuppressive effects and secrete trophic/growth factors that support regenerative processes,<sup>21,22</sup> but do not seem to thrive in the harsh NP environment.<sup>23</sup>

A more logical approach for sustained clinical improvement would be to use NPCs, which are already adapted to the hostile NP environment. Repopulating the degenerated IVD with NPCs has already been shown to promote regeneration in various species.<sup>24–28</sup> Next to that, recent work has detected a population of TEK receptor tyrosine kinase (TEK; also known as TIE2) + NP progenitor cells with regenerative potential which decreases with age and degeneration of the IVD.<sup>29,30</sup> Even in the degenerated IVD progenitor, cells seem to be present in the NP forming cell clusters which express *i.a.* cytokeratin-8 and 19, and cluster of differentiation (CD) cell surface markers typical of stem cells which could be indicative of an attempted repair response.<sup>31</sup> Yet

the applicability of NPCs as a cell-based therapy for LBP has been hampered by *i.a.* the low cell numbers that can be extracted from donor IVDs, and thus, extensive *in vitro* expansion of NPCs is needed to achieve cell numbers that are required for allogeneic cell transplantation. However, primary cells are prone to de-differentiate during *in vitro* expansion lacking tissue-specific stimuli.<sup>10</sup> For NPCs, it is known that their specific morphology and phenotype are not maintained in two-dimensional (monolayer) expansion culture, becoming more fibroblast-like.<sup>32</sup> NPCs are known to lose SOX9 and collagen type II expression already during the first passage.<sup>33</sup> Furthermore, the fraction of TEK+ cells was rapidly lost in monolayer cultures, and low oxygen levels (2%  $O_2$ ) and supplementation with basic fibroblast growth factor (FGF-2) could only partly prevent this.<sup>34</sup> Furthermore, the regenerative capacity of NPCs obtained from herniated and/or degenerated IVDs could be limited unless their degenerated phenotype is reversed. A promising strategy to optimize NPC expansion is to focus on physiological stimuli that influence the NPC phenotype and matrix-producing capacity *in vitro*. The native IVD is a hostile environment, characterized by low oxygen tension, low nutrition, high osmolarity, low pH, and exists under dynamic load.<sup>35,36</sup> Yet the majority of *in vitro* studies are performed in nutrient-rich culture media, at neutral pH (7.4), low osmolality (~350 mOsm/L), and under static culture conditions at 21%  $O_2$ .<sup>10</sup> Recent work showed that increasing the medium osmolarity during expansion, but not during 3D re-differentiation culture, exerted beneficial effects on the regenerative capacity of NPCs of three human donors *in vitro* by improving GAG and collagen type II deposition after hydrogel culture.<sup>37</sup> To date, this has not been tested on dog NPCs, even though dogs are considered a clinically relevant model for IVD regeneration.<sup>38</sup> Similar to humans, they suffer from LBP due to IVD degeneration, show similar pathophysiological processes, and are used for preclinical testing of cell-based therapies to repair the degenerated IVD, and are an important target for veterinary medicine.<sup>38,39</sup> To further understand to what extent the NPC phenotype is modified by adjusting medium osmolarity conditions during expansion, we investigated the effect of increasing expansion medium osmolarity on the phenotype of dog NPCs and their ability to proliferate and produce healthy ECM in a 3D culture model.

## 2 | METHODS

### 2.1 | Experimental setup

The objective of the study was to determine the effect of increasing expansion medium osmolarity from 300 mOsm/L, considered the standard culture medium osmolarity, to hyperosmolar conditions of 400 and 500 mOsm/L during expansion on dog NPCs isolated from mildly to moderately degenerate IVDs. Besides expanding the NPCs in the standardly used oxygen level (normoxia; 21%  $O_2$ ), this was also performed in hypoxia (5%  $O_2$ ). Five percent  $O_2$  levels mimic better the *in vivo* situation of the IVD and are considered as such physioxic for the NP and are reported to better preserve the NPCs' regenerative potential in humans.<sup>40</sup> To assess how the expanded NPCs responded

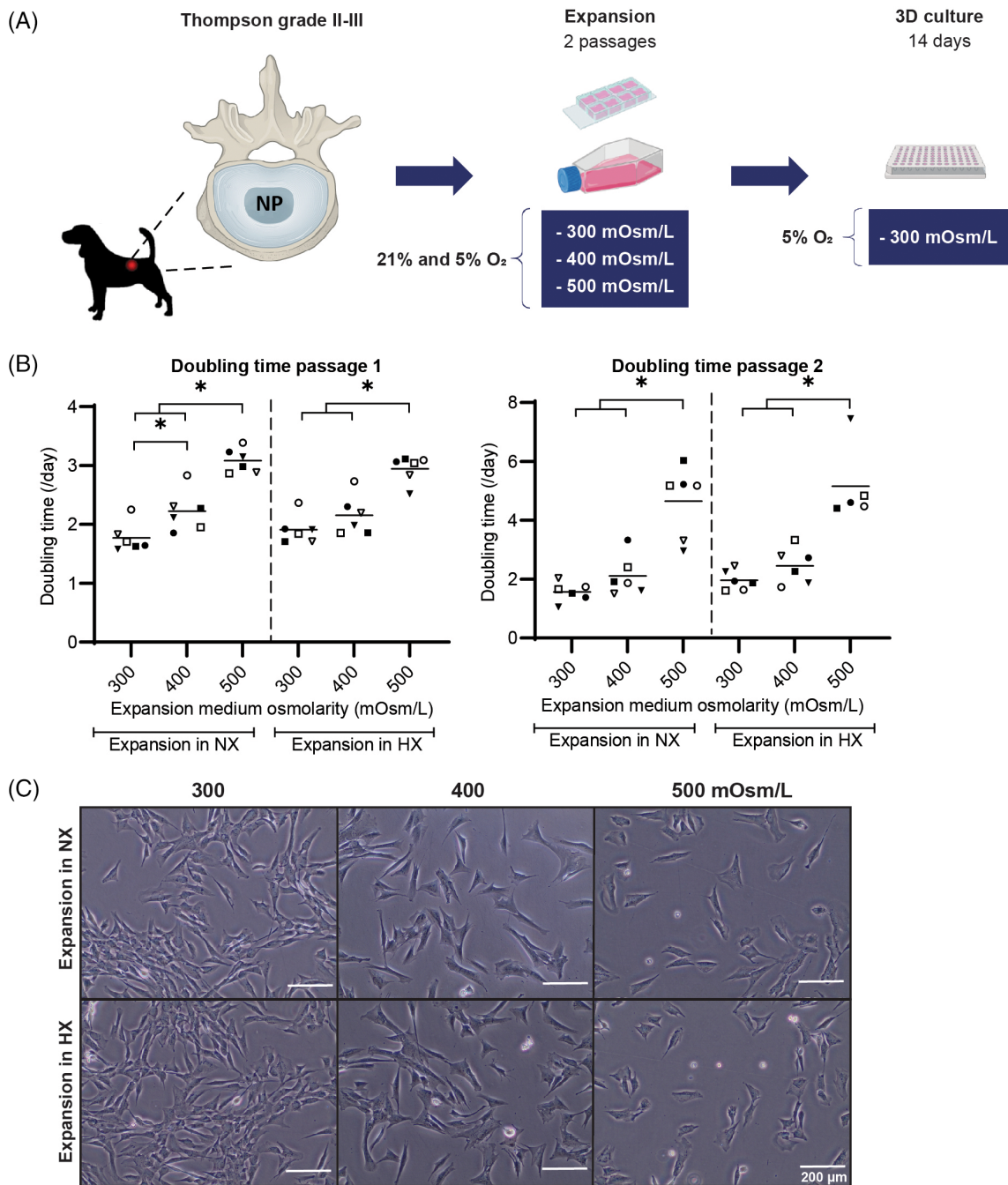


**FIGURE 1** Expansion in 500 mOsm/L results in polygonal nucleus pulposus cells (NPCs) with a lower cell proliferation rate. (A) Experimental design. (B) Population doubling time of the NPCs during Passage 1 to 2 and 2 to 3 when expanded in normoxia (NX: 21% O<sub>2</sub>) and hypoxia (HX: 5% O<sub>2</sub>) in the different media osmolarities (lines indicate the mean ± SD). The black symbols represent female donors and white symbols male donors. \**p* < 0.05 corrected for multiple testing. (C) Representative brightfield images of NPC morphology at Day 3 of expansion in both NX and HX conditions in the different media osmolarities

when placed back in osmolarity levels similar to a degenerated disc, a 3D microaggregate culture model was used with a chondrogenic culture medium of 300 mOsm/L (Figure 1A). NPCs were analyzed for changes in cell phenotype and healthy ECM production capacity by determining cell proliferation rate and morphology, and the gene and protein expression levels of key NPC, progenitor, and ECM-associated markers.

## 2.2 | Isolation of NPCs

Complete dog spines were collected from Beagles euthanized in unrelated ethically approved research studies (Table 1). Beagles are chondrodystrophic dogs in which notochordal cells (NCs) are lost and replaced by NPCs between 3 and 12 months of age comparable to humans in which we also see a complete loss of NCs before adulthood has reached.<sup>42</sup> As

**TABLE 1** Donor details

| Number | Age (years) | Gender | Breed  |
|--------|-------------|--------|--------|
| 1      | 5           | Female | Beagle |
| 2      | 5           | Female | Beagle |
| 3      | 5           | Female | Beagle |
| 4      | 5           | Male   | Beagle |
| 5      | 5           | Male   | Beagle |
| 6      | 5           | Male   | Beagle |

Note: IVDs of beagles >12 months are typically considered to have Thompson grade II–III degeneration.<sup>23,41</sup>

the role of sex in IVD degeneration has not been consistently studied to date, NPCs of an equal amount of male and female donors were included in this study. IVDs were opened under sterile conditions and NP tissue was collected by precise separation from the annulus fibrosus and endplates. The NP tissue was enzymatically digested with 0.15% pronase (11 459 643 001, Roche Diagnostics) for 45 min and 0.15% collagenase type II (4176, Worthington) for 16 h at 37°C.<sup>23</sup> After digestion, the NPCs were cryopreserved at –196°C until further use.

### 2.3 | Cell culture

Cryopreserved P0 NPCs were expanded in medium containing hgDMEM+Glutamax (31966, Invitrogen) with 10% fetal bovine serum (FBS) (16000–044, Life Technologies), 1% penicillin/streptomycin (P/S, P11–010, PAA Laboratories), 0.1 mM ascorbic acid 2-phosphate (Asap, A8960, Sigma-Aldrich), and 1 ng/ml bFGF (PHP105, AbD Serotec) at standard osmolarity (300 mOsm/L<sup>23</sup>) or adjusted to 400 using 1% 5 M NaCl (6404; Merck) and 1% 0.4 M KCl (P4505; Sigma-Aldrich) or to 500 mOsm/L using 2% 5 M NaCl and 2% 0.4 M KCl.<sup>43</sup> The final medium osmolarity was checked with the Gonotec Osmomat 030. The NPCs were expanded in normoxic (21% O<sub>2</sub>) or hypoxic (5% O<sub>2</sub>) conditions and passaged when ~80% confluency was reached. Following two expansion passages, a 3D microaggregate culture system was used, since culturing IVD cells in a 3D environment is known to maintain the phenotype better than 2D cultures.<sup>44</sup> For each expansion condition, 35 000 NPCs were plated in low-adherence cell-repellent surface 96-well plates (650 970, CELLSTAR Greiner Bio-One) in 50 µl basal culture medium: hgDMEM + Glutamax, 1% P/S, 1% Insulin-Transferrin-Selenium (ITS) + premix (354352, Corning Life Sciences), 0.04 mg/ml L-proline (P5607, Sigma-Aldrich), 0.1 mM Asap, 1.25 mg/ml, and 10 ng/ml human recombinant TGF-β<sub>1</sub> (240-B, R&D Systems, Inc.).<sup>45</sup> TGF-β<sub>1</sub> was used during the 3D culture since it is known to promote and maintain the differentiation status of chondrogenic cells.<sup>46,47</sup> The 3D culture was performed at an osmolarity of 300 mOsm/L, mimicking the degenerate IVD<sup>10</sup> and in hypoxic conditions.

### 2.4 | Cell morphology and cell proliferation rate

To assess NPC morphology, brightfield images were taken on Day 3 of expansion. Doubling times within each passage were calculated from the

trend line of the exponential growth phase using the equation:  $T = \ln 2/k$ , where  $k$  is the growth constant and  $T$  is the doubling time in days.

### 2.5 | Gene expression profiling

Gene expression analysis for monolayer expansion cultures was performed after two passages in the different medium osmolarities using 500 000 cells per donor ( $n = 6$ ) and on Day 3 of the 3D microaggregate culture, using a pool of five NPC microaggregates per donor ( $n = 6$ ) and per condition. Cells from monolayer expansion cultures were collected directly into RLT buffer (79216, Qiagen) with 1% β-mercaptoethanol, while the 3D microaggregates were frozen in liquid nitrogen and crushed using pestles (P9951-901, Argos Technologies) before the addition of the lysis buffer. RNA from monolayers was extracted with the RNeasy Mini Kit according to the manufacturer's instructions, whereas for the microaggregated the RNeasy Micro Kit (74004, Qiagen) was used. A DNase (RNase-Free DNase Set, 79254, Qiagen) step was included to ensure DNA removal. cDNA was synthesized using the iScript cDNA Synthesis Kit (170-8891, Bio-Rad) according to the manufacturer's instructions. Primers were designed with PerlPrimer and M-fold was used to check for secondary structure formation.<sup>46</sup> Primer specificity and uniqueness were tested by BLAST.<sup>47</sup> Annealing temperatures were established by performing a temperature gradient PCR on a 16-fold dilution series. Four reference genes were used to normalize the expression of the target genes (Table 2).

RT-qPCR was performed using the iQTM SYBR Green Supermix Kit (Bio-Rad) and the CFX384 Touch Real-Time PCR Detection System (Bio-Rad) (40 cycles; denaturation 95°C, annealing temp (Table 2), extension 65°C). Relative quantification was calculated using the efficiency-corrected  $\Delta\Delta C_T$  method. For each target gene, the  $C_T$ -value was normalized to the mean  $C_T$ -value of the reference genes using the following formula:  $\Delta C_T = C_{T \text{ target}} - C_{T \text{ mean ref}}$ . As calibrator, the universal  $\Delta C_T$ -value of all expansion or 3D culture samples was used. Thereafter, the  $E^{-\Delta\Delta C_T}$ -value for the test and calibrator sample was calculated. In this formula,  $E$  indicates the amplification efficiency (between 95% and 105%) of the target gene.<sup>48</sup>

### 2.6 | Histological analysis

To determine the protein levels of key NPC and progenitor markers after monolayer expansion, cells were seeded at 10 000 cells per well in chamber slides (Millipore, PEZGS0816). After two expansion passages in the different media osmolarities (300, 400, and 500 mOsm/L) and oxygen levels (21% and 5% O<sub>2</sub>), the cells were fixed in 4% neutral buffered formaldehyde for 10 minutes. Immunofluorescent (IF) staining was performed for NPC markers PAX1, ACAN, and CD24 and progenitor markers TEK and CD73. For this, the slides were first incubated with 3% BSA in 0.1% Triton-X 100 (37240, Serva) for 1 h to permeabilize the cells and block unspecific binding sites. After two washing steps with PBS, the slides were incubated overnight at 4°C with the primary antibodies (Table 3) diluted in 1% BSA in PBS. After washing with PBS,

**TABLE 2** Primer information for reference and target genes

| Genes   | Forward sequence 5' → 3' | Reverse sequence 5' → 3' | Annealing temperature (°C) |
|---------|--------------------------|--------------------------|----------------------------|
| RPL13   | GCCGGAAGTTGTAGTCGT       | GGAGGAAGGCCAGGTAATTC     | 61                         |
| RPS19   | CCTTCTCAAAAAGTCTGGG      | GTTCTCATCGTAGGGAGCAAG    | 61                         |
| SDHA    | GCCTTGATCTCTTGATGGA      | TTCTTGCTCTTATGCGATG      | 61                         |
| TBP     | CTATTCTTGGTGTGCATGAGG    | CCTCGCATTAGTCTTTTC       | 57                         |
| ACAN    | GGACTCCTTGAATTTGAG       | GTCATTCCACTCTCCCTTCTC    | 62                         |
| COL2A1  | GCAGCAAGAGCAAGGAC        | TTCTGAGAGCCCTCGGT        | 62                         |
| COL1A1  | TCCAACGAGATCGAGATCC      | AAGCCGAATTCCTGGTCT       | 61                         |
| ADAMTS5 | CTACTGCACAGGGAAGAG       | GAACCCATTCCACAAATGTC     | 61                         |
| MMP13   | CTGAGGAAGACTTCCAGCTT     | TTGGACCACTTGAGAGTTCG     | 65                         |
| CCND1   | GCCTCGAAGATGAAGGAGAC     | CAGTTTGTCCACCAGGAGCA     | 60                         |
| BAX     | CCTTTTGCTTCAGGGTTTCA     | CTCAGCTTCTGGTGGATGC      | 58                         |
| BCL-2   | ATCGCCTGTGGATGACTGAG     | CAGCCAGGAGAAATCAAACAGAGG | 64                         |
| CASP3   | CGGACTTCTTGATGCTTACTC    | CACAAAGTACTGGATGAACC     | 61                         |
| p27     | CGGAGGGACGCCAAACAGG      | GTCCCGGTCAACTCTTCGTG     | 68                         |
| FOXF1   | GAGTTCGTCTTCTCCTTCAACAC  | GCTTGATGTCTTGGTAGGTGAC   | 58                         |
| KRT8    | CCTTAGCGGGTCTCTCGTA      | GGGAAGCTGGTGTCTGAGTC     | 63                         |
| KRT18   | TTGCTACTACCGTCGCTGTTGG   | ATCTTGCGGGTGGTGGTCTTCTGG | 63.5                       |
| KRT19   | GCCCAGCTGAGCGATGTGC      | TGCTCCAGCCGTGACTTGATGT   | 64                         |
| CA12    | CTAGAGAAATGGTCAACAACCTCC | CACAGATGCCAAGAACGC       | 58.5                       |
| T       | CTGAACTCCTTACATAAGTACGAG | GCTGTGATCTCTCATTCTG      | 62.5                       |
| TEK     | CAGCTTACCAGGTGGACATTTTTG | GTCCGCTGGTCTTGAGATTTAG   | 58                         |
| ANG1    | AATAATATGCCAGAACCACAAAAG | CCCCAGCAATATTCACCAGAG    | 62                         |
| CD24    | GGGACAAATCCAGCAGAAAA     | TACAGAGCCTGGAGCTGGTT     | 66                         |
| CD44    | CTTCTGCAGATCCGAACACA     | GAGTAGAAGCCGTTGGATGG     | 60                         |
| CD73    | CTCCAACACATTCTTTACAC     | ACTCAACCTTCAAATAGCCT     | 61                         |
| CD105   | CATCCTTACCACCAAGAG       | CAGATTGCAGAAGGACGG       | 60                         |
| NFAT5   | TTTATGTACTCAGCCAGCAGG    | ATACTTCTTCTCTCTTCACTG    | 63.5                       |

the slides were incubated for 1 h with the appropriate secondary antibody diluted in 1% BSA in PBS in the dark. Thereafter, the slides were washed and nuclear counterstaining was performed with DAPI Solution (62248, Thermo Fisher Scientific) for 5 min. Slides were imaged using the LEICA TCS SP8 X. (Positive) cell numbers were manually counted in three fields ( $\times 400$  magnification) per well using Photoshop CC and the percentage of positive cells was calculated per donor. For histological evaluation after the 3D culture, microaggregates ( $n = 3$  replicates per donor and condition) on Day 14 of microaggregate culture were embedded in agarose, fixed in 4% neutral buffered formaldehyde for 16 h, and, after a graded ethanol series, embedded in paraffin. Tissue sections ( $5 \mu\text{m}$ ) were used to evaluate matrix deposition with Safranin O/Fast Green staining and an immunohistochemical (IHC) staining for COL2 and ACAN as described previously using the DAB chromogen.<sup>45</sup> To determine the protein levels of NPC and progenitor markers, IHC staining for PAX1, CD24, TEK, and CD73 was performed using specific antigen retrieval steps, provided in Table 3. Rabbit (37415, Abcam) and mouse IgG (X0931, Dako) were used as isotype controls at the same concentration as the primary antibodies. Details of the antibodies and protocols of the IHC (first rows) and IF staining (second rows) are provided in Table 3.

## 2.7 | Biochemical analysis

For determining the glycosaminoglycan (GAG) and DNA content, microaggregates ( $n = 3$  replicates per donor and condition) were collected on Day 14 of the 3D culture. The DNA and GAG content was measured as described previously using the Qubit dsDNA High Sensitivity Assay Kit (Q32851, Invitrogen) and a dimethyl methylene blue (DMMB) assay, respectively.<sup>45</sup>

## 2.8 | Statistical analysis

IBM SPSS statistics 25 was used for statistical analysis. The effects of osmolarity and oxygen were analyzed separately, meaning that each comparison included only one variable. The normality of data was assessed using the Shapiro–Wilk's test. General linear regression models based on analyses of variance were used for normally distributed data, whereas Kruskal–Wallis and Mann–Whitney  $U$  tests were performed on non-normally distributed data. To correct for multiple comparisons, all tests were followed by a Benjamini & Hochberg False

**TABLE 3** Antibody and protocol details of immunohistochemistry (first rows) and immunofluorescence (second rows)

| Name  | Host   | Concentration                | Antigen retrieval                         | Secondary antibody   |
|---|--------|------------------------------|---|--|
| ACAN (ab3778, Abcam)                                  | Mouse  | 11.92 µg/ml                  | Pronase + Hyaluronidase (60 min, 37°C)    | Brightvision Poly-HRP Anti-Mouse (VWRKDPVM110HRP, Immunologic)               |
|   |        | 11.92 µg/ml                  | Triton-X 100 (0.1%) (60 min, RT)          | Goat Anti-Mouse IgG, Alexa Fluor Plus 488 (A32723, Thermo Fisher Scientific) |
| CD24 (LS-C87657, LSBio)                               | Mouse  | 1:200<br>(concentration N/A) | 0.01 M citrate buffer pH 6 (60 min, 70°C) | Brightvision Poly-HRP Anti-Mouse   |
|   |        | 1:100                        | Triton-X 100 (0.1%) (60 min, RT)          | Goat Anti-Mouse IgG, Alexa Fluor Plus 488                                    |
| CD73 (LS-B8284, LSBio)                                | Rabbit | 0.5 µg/ml                    | none                                      | BrightVision Poly-HRP Anti-Rabbit (VWRKDPVR110HRP, Immunologic)              |
|   |        | 5 µg/ml                      | Triton-X 100 (0.1%) (60 min, RT)          | Donkey Anti-Rabbit IgG, Alexa Fluor 594 (A21207, Thermo Fisher Scientific)   |
| COL2 (II-II6B3, Developmental Studies Hybridoma Bank) | Mouse  | 0.03 µg/ml<br>N/A            | Pronase + Hyaluronidase (30 min, 37°C)    | Brightvision Poly-HRP Anti-Mouse   |
| PAX1 (ab203065, Abcam)                                | Rabbit | 4 µg/ml                      | 0.01 M citrate buffer pH 6 (30 min, 70°C) | BrightVision Poly-HRP Anti-Rabbit  |
|   |        | 10 µg/ml                     | Triton-X 100 (0.1%) (60 min, RT)          | Donkey Anti-Rabbit IgG Alexa Fluor 594                                       |
| TEK (sc-324, Santa Cruz Biotechnology)                | Rabbit | 4 µg/ml                      | 0.01 M citrate buffer pH 6 (30 min, 70°C) | BrightVision Poly-HRP Anti-Rabbit  |
|   |        | 4 µg/ml                      | Triton-X 100 (0.1%) (60 min, RT)          | Donkey Anti-Rabbit IgG Alexa Fluor 594                                       |

Discovery Rate post hoc test.  $p$  Values <0.05 were considered significant.

### 3 | RESULTS

#### 3.1 | Increasing medium osmolarity affects NPC morphology and proliferation rate

To investigate the effects of culture medium osmolarity on monolayer expansion, NPCs from degenerated IVDs of six Beagle donors were expanded for two passages in normoxic (21% O<sub>2</sub>) or hypoxic (5% O<sub>2</sub>) conditions in an expansion medium with a standard osmolarity of 300 mOsm/L or adjusted to 400 or 500 mOsm/L (Figure 1A). Increasing osmolarity up to 500 mOsm/L during expansion resulted in a significant ( $p < 0.05$ ) increase in population doubling time during both expansion passages regardless of the oxygen levels (Figure 1B). Furthermore, increased medium osmolarity to 400 mOsm/L significantly increased the population doubling time in normoxia during the first passage (Figure 1B). In NPCs expanded in 500 mOsm/L, gene expression of senescence marker *p27* significantly increased compared to 300 mOsm/L only in normoxic conditions, whereas no significant differences were detected for pro-apoptotic markers *CASP3* and *BAX*, and anti-apoptotic marker *BCL2* (Figure S1). Expression of proliferation marker *CCND1* was not detectable. In terms of morphology, dog NPCs expanded in 300 mOsm/L, in both normoxia and hypoxia, appeared spindle-shaped, stretched out, and flattened with long filopodia as commonly reported for monolayer culture of NPCs

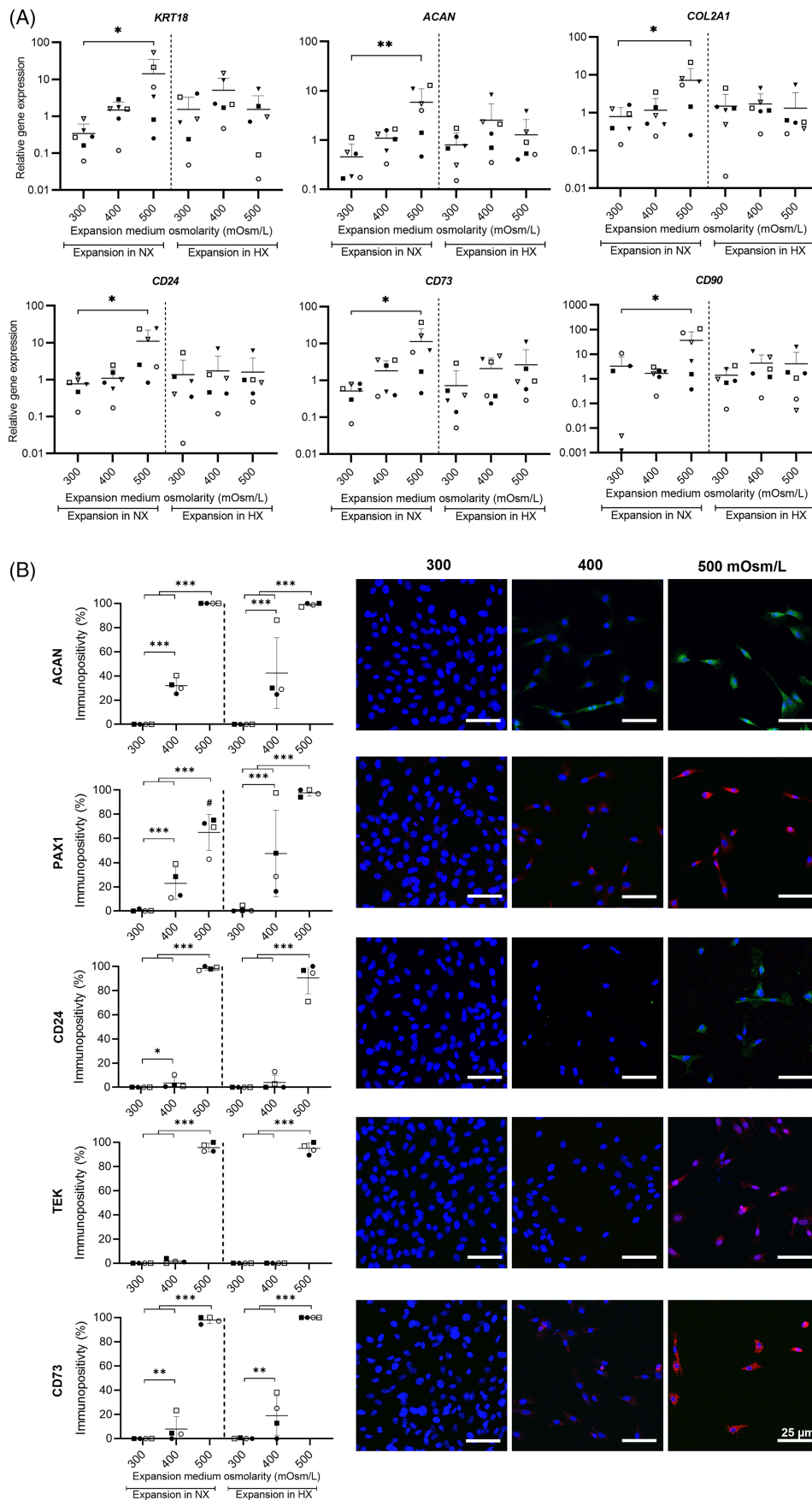
(Figure 1C).<sup>32</sup> In contrast, NPCs that expanded in 400 and 500 mOsm/L appeared more polygonal, with shorter filopodia (Figure 1C).

#### 3.2 | Hyperosmolar expansion medium improves dog nucleus pulposus cell phenotype

We next sought to explore the effect of medium osmolarity on the NPC phenotype during expansion via gene expression profiling following two passages in normoxic and hypoxic conditions. Increasing the expansion medium osmolarity to 500 mOsm/L significantly increased gene expression of NPC markers *ACAN*, *COL2A1*, *KRT18*, and *CD24* (Figure 2A) which are typically expressed in non-degenerated IVDs,<sup>49</sup> and progenitor markers *CD73* and *CD90*<sup>30</sup> in normoxic conditions (Figure 2A); a change not seen in hypoxic conditions. The expression of NPC markers *KRT8*, *FOXF1*, and progenitor marker *CD105*<sup>30</sup> remained unchanged, regardless of oxygen level (Figure S2). In contrast to the other NPC markers, the expression of *CA12* was significantly decreased in 500 mOsm/L compared to expansion in the lower osmolarities (Supp Figure 2). While gene expression of the progenitor marker *TEK*<sup>30</sup> was undetectable in all conditions, the expression of its ligand *ANG1*<sup>29,34</sup> was significantly increased in the NPCs expanded in 500 mOsm/L under normoxic conditions. No significant differences in the expression of osmosensitive marker *NFAT5* were detected (Figure S2).

Because gene expression levels do not always directly correlate with protein levels,<sup>50</sup> we complemented the analysis with

**FIGURE 2** Hyperosmolar expansion medium improves the phenotype of dog nucleus pulposus cells (NPCs) independent of oxygen level. (A) Fold changes in relative gene expression of NPC and progenitor markers after expansion of two passages in both normoxic (NX: 21% O<sub>2</sub>) and hypoxic (HX: 5% O<sub>2</sub>) conditions in the different media osmolarities (lines indicate the mean + SD). The black symbols represent female donors and white symbols represent male donors. \**p* < 0.05 corrected for multiple testing. (B) Immunofluorescence images and quantification for ACAN, PAX1, CD24, TEK, and CD73 protein levels following expansion for two passages in the different media osmolarities in HX (lines indicate the mean ± SD). The black symbols represent female donors and white symbols represent male donors. \*\**p* < 0.01, \*\*\**p* < 0.001, #significantly different (*p* < 0.05) from expansion in HX using the same medium osmolarity corrected for multiple testing



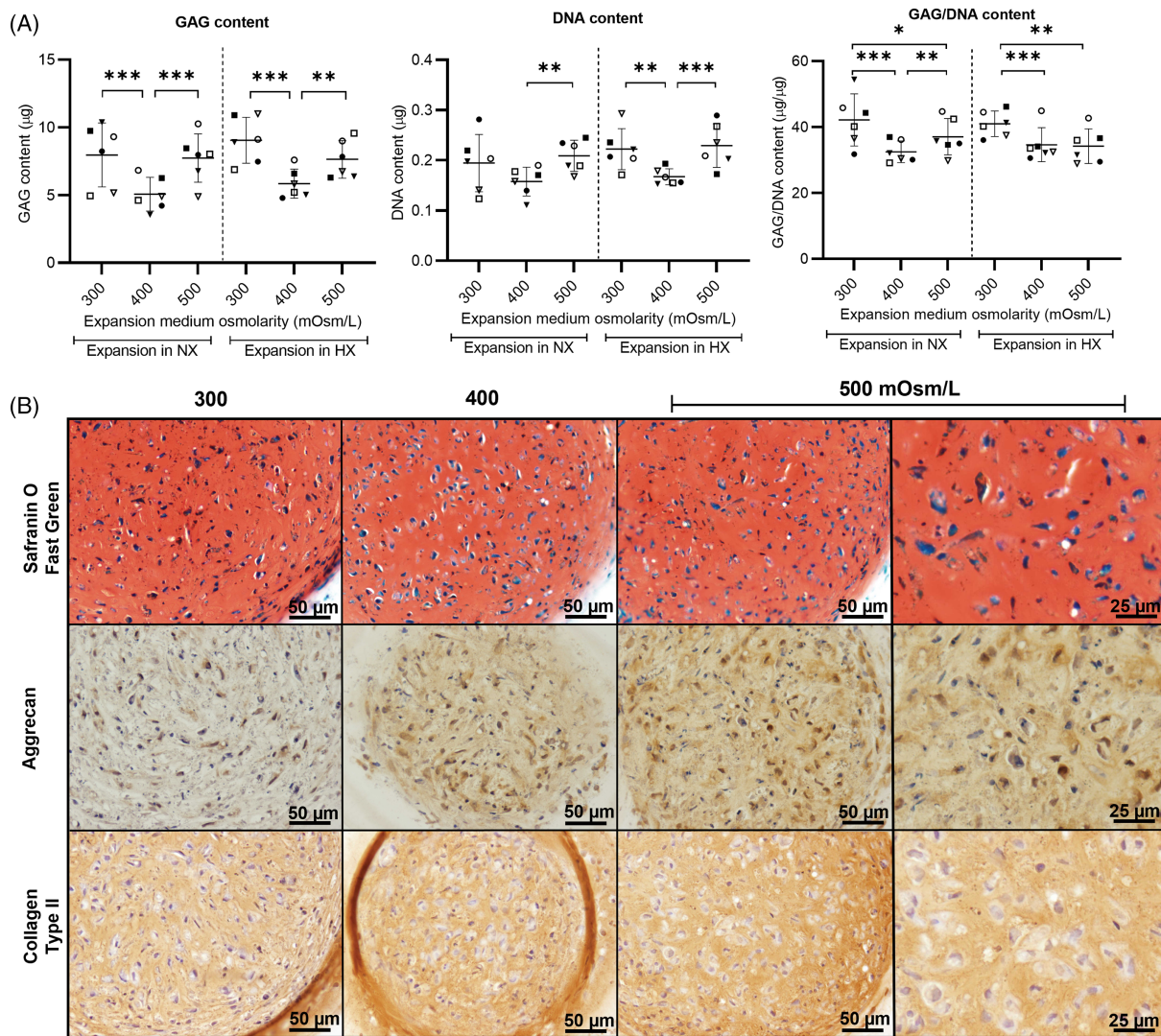


**FIGURE 3** Hyperosmolar expansion medium maintains healthy ECM production and deposition during 3D culture. (A) GAG and DNA content of the nucleus pulposus cell (NPC) microaggregates at Day 14 of 3D culture (300 mOsm/L; 5% O<sub>2</sub>) after expansion in both normoxic (NX; 21% O<sub>2</sub>) and hypoxic (HX; 5% O<sub>2</sub>) conditions in the different media osmolarities (300, 400, and 500 mOsm/L; lines indicate the mean ± SD). The black symbols represent female donors and white symbols represent male donors (mean of two technical replicates). \**p* < 0.05, \*\**p* < 0.01, \*\*\**p* < 0.001 corrected for multiple testing. (B) Safranin O/Fast Green and immunohistochemical staining for aggrecan and collagen type II of the NPC microaggregates collected at Day 14 of 3D culture (300 mOsm/L; 5% O<sub>2</sub>) after expansion in HX conditions in the different media osmolarities

immunofluorescence for a subset of markers. In line with the gene expression, the protein levels of NPC markers ACAN and CD24 and progenitor marker CD73 were significantly increased when NPCs were expanded in 500 mOsm/L compared to 300 mOsm/L in normoxic conditions. In contrast, these protein levels were also increased in hypoxic expansion conditions (Figure 2B). Furthermore, protein levels of NPC markers PAX1 and progenitor marker TEK were also significantly increased when NPCs were expanded in 500 mOsm/L compared to the lower osmolarity conditions, under both normoxic and hypoxic conditions (Figure 2B). This indicates that increased expansion medium osmolarity exerted a beneficial effect on the dog NPCs phenotype.

### 3.3 | Hyperosmolar expansion medium maintains ECM production and deposition in 3D culture

To assess the capacity of the NPCs expanded in the different conditions to produce healthy ECM, NPCs of all expansion conditions were afterward cultured in 3D microaggregates in standard medium osmolarity under hypoxic conditions in the presence of chondro-permissive medium with 10 ng/ml TGF-β<sub>1</sub> supplementation. In this way, the NPCs expanded in the higher osmolarities were challenged by placing them back into the osmolarity level present in a degenerated IVD. To investigate how the expanded NPCs responded to this change in osmolarity, we performed RT-qPCR on Day 3 of the 3D culture.



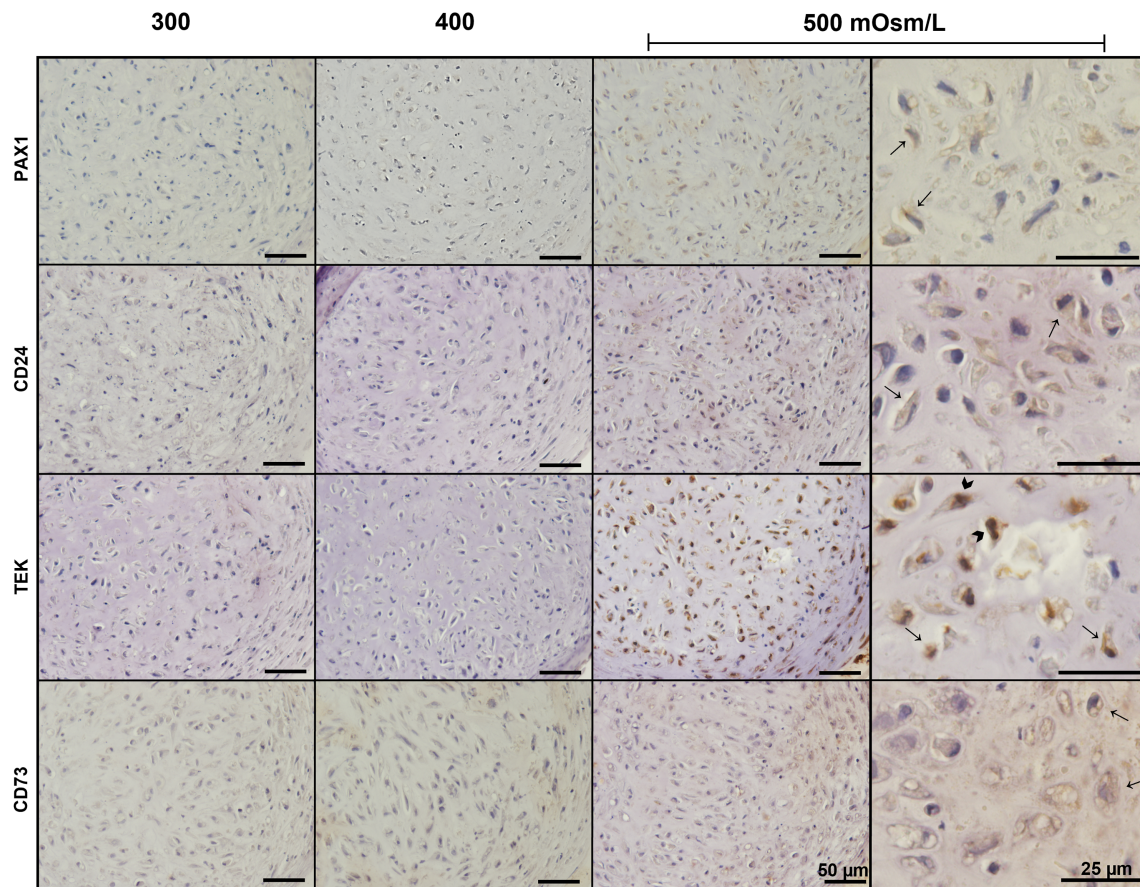


**FIGURE 4** Nucleus pulposus cells (NPCs) expanded in higher osmolarity retain the expression of healthy phenotypic markers during 3D culture. Immunopositivity for PAX1, CD24, TEK, and CD73 at Day 14 in NPC microaggregates collected at Day 14 of 3D culture (300 mOsm/L; 5% O<sub>2</sub>) after expansion in hypoxic conditions in the different media osmolarities. Arrows indicate extracellular matrix, cytoplasmic/membranous and arrow heads indicate nuclear localization of immunopositivity.

However, no significant differences between any osmolarity conditions were detected in the expression of genes involved in ECM production and remodeling (Figure S3).

To further assess the performance of the NPC microaggregates, they were analyzed for DNA content and their ability to produce GAGs at Day 14 of 3D culture (Figure 3A). While the proliferation rate during expansion was significantly lower in NPCs expanded in 500 mOsm/L conditions in both hypoxia and normoxia (Figure 1B), the NPC microaggregates expanded in 500 mOsm/L contained a similar DNA content compared to microaggregates expanded in 300 mOsm/L (Figure 3A). Notably, the two extreme osmolarity conditions showed no significant differences in GAG and DNA content, while a significantly higher GAG and DNA content was observed compared to expansion in 400 mOsm/L, an effect seen for NPCs expanded in both oxygen levels (Figure 3A). Following 14 days in 3D culture, in all NPC microaggregates diffuse and intense Safranin O staining was observed, indicating proteoglycan deposition (Figure 3B). While aggrecan immunostaining was present in all osmolarity levels, in line with expression levels during the expansion phase (Figure 2B), the expression was highest in NPC microaggregates expanded at 500 mOsm/L showing both intracellular and ECM staining (Figure 3B).

In all conditions, the ECM was also immunopositive for type II collagen.

### 3.4 | NPCs expanded in higher osmolarity retain the expression of healthy phenotypic markers during 3D culture

To assess whether the NPCs expanded in increased medium osmolarity were able to retain the expression of healthy NPC and progenitor markers in 3D culture at osmolarity levels comparable to the degenerate disc, gene and protein levels were determined for the same subset of markers as selected for expansion. Only gene expression of progenitor marker *CD73* appeared to be increased in NPCs that had been expanded in both 400 and 500 mOsm/L under hypoxic conditions (Figure S4). We next evaluated protein levels in the microaggregates following the 14 days of 3D culture with IHC staining for PAX1, CD24, TEK, and CD73 (Figure 4). Immunopositivity for PAX1 was only detected in the cytoplasm (arrows) of NPCs expanded at 500 mOsm/L. Furthermore, only the NPCs expanded in 500 mOsm/L showed CD24 staining in the cytoplasm/cell membrane (arrows). In contrast to

the other osmolarity conditions, TEK was prominently detected in both the cytoplasm/cell membrane (arrows) and nuclei (arrowheads) of the NPCs expanded in 500 mOsm/L, while membranous staining (arrows) of CD73 was detected in the NPCs expanded at 500 mOsm/L.

## 4 | DISCUSSION

The present study investigated the effects of increasing culture medium osmolarity during expansion on the phenotype of dog NPCs and their performance in a 3D culture model. We show that expansion in culture medium osmolarity that mimics the healthy IVD environment enhances the gene expression and protein levels of several healthy NPC and progenitor markers at the expense of the proliferation rate. These expanded NPCs maintained healthy ECM deposition when cultured in a 3D culture model mimicking degenerated osmolarity levels. Comparable responses in terms of ECM production reported in human NPCs expanded under hyperosmolar conditions confirm the suitability of the dog as a clinical model for the development of new treatments for IVD regeneration.<sup>37</sup>

### 4.1 | Hyperosmolar expansion conditions direct degenerated NPCs to a more progenitor-like and healthy phenotype

Our results suggest that expansion in hyperosmolar conditions could direct the degenerated NPCs to a more progenitor-like and healthy phenotype. While there is no consensus on a set of phenotypic markers that can identify healthy NPCs, we focused on ACAN, PAX1, and CD24 expression as known markers of a healthy human IVD recently reviewed by Bach et al.<sup>42</sup> Gene and protein levels of these NPC markers were increased following expansion in 500 mOsm/L. Given that high levels of CD24 are seen in the fetal NP,<sup>51</sup> this suggests that hyperosmolar conditions result in NPCs with a young and healthy phenotype. Further, protein levels of progenitor markers TEK and CD73 and gene expression of *CD73* and *CD90* were significantly increased after expansion at 500 mOsm/L. TEK is identified as a marker of the local NP progenitor cell population in several species<sup>29,30</sup> and CD73 and CD90 are known as MSC markers and indicative of stem cell activity in the degenerated IVD.<sup>31</sup> The increased ACAN and COL2 gene expression after expansion also implies a positive effect of the hyperosmolar conditions in the ability to produce healthy NP matrix production.

This study shows that during the 3D culture in hypo-osmolar conditions, mimicking the levels in the degenerated IVD, the improved NPC phenotype was maintained. Next to that, increasing the expansion medium osmolarity up to 500 mOsm/L retained the ability to produce healthy ECM of the NPCs indicated by the similar quantity of GAG production compared to standard medium osmolarity. Unexpectedly, in 3D culture, a significantly decreased GAG and DNA content were seen in NPCs expanded in 400 mOsm/L compared to 300 and

500 mOsm/L. As technical errors were excluded, further research is needed to explain this deviant finding. Although collagen type II deposition seemed similar between conditions, the increased aggrecan immunopositivity of the NPC microaggregates expanded in the higher osmolarity conditions indicates that the quality of the ECM was potentially improved.<sup>52</sup> Since the use of TGF- $\beta_1$  could have masked differences in the regenerative capacity of the NPCs after expansion in the different conditions, this should be further investigated without the addition of growth factors and using a culture model that better mimics the in vivo (degenerated) IVD environment e.g. by using hydrogels, NP tissue explants, and the addition of cytokines.<sup>10,53,54</sup> Indeed, human NP cells cultured in several types of hydrogel in the absence of TGF- $\beta$ , showed enhanced ECM production when expanded in hyperosmolar conditions.<sup>37</sup> As the role of sex in IVD degeneration has not been consistently studied to date, NPCs of an equal amount of male and female donors were included in this study. Our data show no significant differences between the male and female donors indicating that NPCs of both sexes respond similar to increasing expansion medium osmolarity. However, since this study was performed in vitro, the effects of sex hormones<sup>55</sup> are not taken into account and should therefore be further investigated in in vivo models.

### 4.2 | Improved NPC phenotype is accompanied by a lower proliferation rate

Together with the beneficial effects on the NPC phenotype, the increased medium osmolarity resulted in a significantly lower cell proliferation rate during expansion. This is in line with previous work which also reported that hyperosmotic treatment reduced bovine NPC proliferation.<sup>56</sup> Since NPCs within the healthy IVD also show little evidence of cell division and are sparsely distributed as single or occasional doublet cells in an extensive ECM, the lower proliferation rates are not unexpected.<sup>57</sup> Also, NPC proliferation is considered to be associated with IVD degeneration and an attempt for a regenerative response likely leads to the appearance of NPC clusters.<sup>57</sup> To mitigate the effects of increased osmolarity on proliferation and obtain sufficient cell numbers for cell-based therapies, medium osmolarity levels can be more gradually increased, or cells could be first expanded in standard medium osmolarity to obtain sufficient cells and thereafter exposed to the increased medium osmolarity to improve the NPC phenotype.

### 4.3 | Adjusting osmolarity during expansion outperforms the effect of physioxia

Adjusting osmolarity during expansion seems to outperform the effect of adjusting oxygen levels to the native NP environment, that is, physioxia. The healthy IVD environment is hypoxic with  $pO_2$  ranging from 1% to 5%  $O_2$ ,<sup>6,7</sup> while standard expansion cultures are routinely carried out at higher oxygen levels of 21%  $O_2$ . Therefore, we assessed

the effects of increasing medium osmolarity under both normoxic and hypoxic expansion conditions. The expression of senescence marker p27 was significantly higher in normoxia compared to hypoxia in the 500 mOsm/L expansion condition (Figure S1), which could potentially be caused by hyper-osmolarity environment-induced oxidative stress injury.<sup>58</sup> This was not seen in the hypoxic environment which is reported to inhibit cell senescence.<sup>59</sup> Although the increased gene expression of phenotypic markers was mainly detected under normoxic expansion conditions, the effects at the protein level were comparable for the two oxygen levels. In contrast, previous work indicated that isolation, expansion, and culture of human NPCs at 3.5% O<sub>2</sub> could better preserve the regenerative potential, showing higher expression of ACAN and COL2.<sup>40</sup> Further, the depletion of ACAN and COL2 after isolation and expansion under normoxic conditions was reported to be partially rescued by later hypoxic cultivation in monolayers.<sup>40</sup> Indeed, since all expanded dog NPCs were cultured after expansion under a hypoxic 3D model to mimic pO<sub>2</sub> in degenerative discs in the present study, this could have potentially masked the effect on gene expression levels induced by expansion in different oxygen levels. Altogether, our results indicate that the effect of increasing medium osmolarity during expansion dominates that of decreasing the oxygen level.

The precise molecular mechanism by which osmolarity exerts this effect in NPCs is still poorly understood and mechanisms by which increases in osmolarity lead to the beneficial phenotypic changes in the present study remain to be elucidated. However, it is known that the nuclear factor of activated T-cells 5 (NFAT5) plays a key role in the mammalian hypertonic stress response as evidenced by the increase in mRNA expression of NFAT5 in several cell types in response to hypertonicity.<sup>60–63</sup> Work from Krouwels et al.<sup>64</sup> and Gajghate et al.<sup>65</sup> show that this increased NFAT5 expression is also involved in human NPCs exposed to hyperosmolar conditions, regulating the expression of tonicity-dependent water channel aquaporin 2. In this study, NFAT5 gene expression was not significantly upregulated in the NPCs expanded at higher osmolarity (Figure S2) but its transient upregulation was possibly missed at the selected time point. Osmolarity responses in human IVD cells have also been shown to be regulated by aquaporin channels and the Transient Receptor Potential Cation Channel Subfamily V Member 4, regulating alterations in cell volume.<sup>66</sup> Thus, the further relationships between these regulatory mechanisms and the improved phenotype of the NPCs observed in hyperosmolar expansion conditions warrant further investigation.

## 5 | CONCLUSIONS

Repopulating the NP using advanced cell-based therapies is becoming an attractive alternative for treating mild to moderate IVD degeneration and preventing progression to severe IVD disease requiring invasive surgery. NPCs that are already adapted to the hostile environment of the IVD are considered potential cell candidates. Our data show that expansion of dog NPCs in higher osmolarity promotes gene expression and protein levels of healthy NPC and progenitor

markers. This population with improved NPC phenotype could have the potential to exert regenerative effects when injected into degenerated IVDs and would therefore be beneficial for cell-based therapies. Altogether, we expect that future studies on mitigating the effects of higher osmolarity on cell proliferation rates will make NPCs a powerful addition to the regenerative toolbox for IVD degeneration.

## ACKNOWLEDGMENTS

This project has received funding from the European Union's Horizon 2020 research and innovation programme under grant agreement no. 825925 and the Dutch Arthritis Society (LLP12 and LLP22). The authors would like to thank Annelinde Voordijk for helping with the execution of experiments.

## CONFLICT OF INTEREST

The authors declare no conflicts of interest.

## ORCID

Lisanne T. Laagland  <https://orcid.org/0000-0002-4456-6167>

Laura B. Creemers  <https://orcid.org/0000-0002-1585-3052>

Christine L. Le Maitre  <https://orcid.org/0000-0003-4489-7107>

Marianna A. Tryfonidou  <https://orcid.org/0000-0002-2333-7162>

## REFERENCES

- Clark S, Horton R. Low back pain: a major global challenge. *Lancet*. 2018;391:2302.
- Wu A, March L, Zheng X, et al. Global low back pain prevalence and years lived with disability from 1990 to 2017: estimates from the Global Burden of Disease Study 2017. *Ann Transl Med*. 2020;8:299.
- Freemont AJ. The cellular pathobiology of the degenerate intervertebral disc and discogenic back pain. *Rheumatology*. 2009;48:5-10.
- Luoma K, Riihimäki H, Luukkainen R, et al. Low back pain in relation to lumbar disc degeneration. *Spine*. 2000;25:487-492.
- Cheung KM, Samartzis D, Karppinen J, et al. Are "patterns" of lumbar disc degeneration associated with low back pain?: new insights based on skipped level disc pathology. *Spine*. 2012;37:E430-E438.
- Chen JW, Li B, Yang YH, Jiang SD, Jiang LS. Significance of hypoxia in the physiological function of intervertebral disc cells. *Crit Rev Eukaryot Gene Expr*. 2014;24:193-204.
- Soukane DM, Shirazi-Adl A, Urban JP. Analysis of nonlinear coupled diffusion of oxygen and lactic acid in intervertebral discs. *J Biomech Eng*. 2005;127:1121-1126.
- Bergknut N, Smolders LA, Grinwis GC, et al. Intervertebral disc degeneration in the dog. Part 1: anatomy and physiology of the intervertebral disc and characteristics of intervertebral disc degeneration. *Vet J*. 2013;195:282-291.
- Haefeli M, Kalberer F, Saegesser D, Nerlich AG, Boos N, Paesold G. The course of macroscopic degeneration in the human lumbar intervertebral disc. *Spine*. 2006;31:1522-1531.
- Thorpe AA, Bach FC, Tryfonidou MA, et al. Leaping the hurdles in developing regenerative treatments for the intervertebral disc from preclinical to clinical. *JOR Spine*. 2018;1:e1027.
- Le Maitre CL, Freemont AJ, Hoyland JA. The role of interleukin-1 in the pathogenesis of human intervertebral disc degeneration. *Arthritis Res Ther*. 2005;7:R732-R745.
- Wang C, Yu X, Yan Y, et al. Tumor necrosis factor-alpha: a key contributor to intervertebral disc degeneration. *Acta Biochim Biophys Sin*. 2017;49:1-13.

13. Masuda K. Biological repair of the degenerated intervertebral disc by the injection of growth factors. *Eur Spine J.* 2008;17(suppl 4):441-451.
14. Nishida K, Kang JD, Gilbertson LG, et al. Modulation of the biologic activity of the rabbit intervertebral disc by gene therapy: an in vivo study of adenovirus-mediated transfer of the human transforming growth factor beta 1 encoding gene. *Spine.* 1999;24:2419-2425.
15. Aguiar DJ, Johnson SL, Oegema TR. Notochordal cells interact with nucleus pulposus cells: regulation of proteoglycan synthesis. *Exp Cell Res.* 1999;246:129-137.
16. Sakai D. Future perspectives of cell-based therapy for intervertebral disc disease. *Eur Spine J.* 2008;17(suppl 4):452-458.
17. Smith LJ, Silverman L, Sakai D, et al. Advancing cell therapies for intervertebral disc regeneration from the lab to the clinic: recommendations of the ORS spine section. *JOR Spine.* 2018;1:e1036.
18. Williams RJ, Tryfonidou MA, Snuggs JW, le Maitre CL. Cell sources proposed for nucleus pulposus regeneration. *JOR Spine.* 2021;4:e1175.
19. Barakat AH, Elwell VA, Lam KS. Stem cell therapy in discogenic back pain. *J Spine Surg.* 2019;5:561-583.
20. Loibl M, Wuertz-Kozak K, Vadala G, Lang S, Fairbank J, Urban JP. Controversies in regenerative medicine: should intervertebral disc degeneration be treated with mesenchymal stem cells? *JOR Spine.* 2019;2:e1043.
21. Bartholomew A, Sturgeon C, Siatskas M, et al. Mesenchymal stem cells suppress lymphocyte proliferation in vitro and prolong skin graft survival in vivo. *Exp Hematol.* 2002;30:42-48.
22. Tse WT, Pendleton JD, Beyer WM, Egalka MC, Guinan EC. Suppression of allogeneic T-cell proliferation by human marrow stromal cells: implications in transplantation. *Transplantation.* 2003;75:389-397.
23. Bach FC, Tellegen AR, Beukers M, et al. Biologic canine and human intervertebral disc repair by notochordal cell-derived matrix: from bench towards bedside. *Oncotarget.* 2018;9:26507-26526.
24. Hohaus C, Ganey TM, Minkus Y, Meisel HJ. Cell transplantation in lumbar spine disc degeneration disease. *Eur Spine J.* 2008;17(suppl 4):492-503.
25. Meisel HJ, Siodla V, Ganey T, Minkus Y, Hutton WC, Alasevic OJ. Clinical experience in cell-based therapeutics: disc chondrocyte transplantation a treatment for degenerated or damaged intervertebral disc. *Biomol Eng.* 2007;24:5-21.
26. Nomura T, Mochida J, Okuma M, Nishimura K, Sakabe K. Nucleus pulposus allograft retards intervertebral disc degeneration. *Clin Orthop Relat Res.* 2001;389:94-101.
27. Nishimura K, Mochida J. Percutaneous reinsertion of the nucleus pulposus. An experimental study. *Spine.* 1998;23:1531-1538.
28. Ciapetti G, Granchi D, Devescovi V, et al. Ex vivo observation of human intervertebral disc tissue and cells isolated from degenerated intervertebral discs. *Eur Spine J.* 2012;21(suppl 1):S10-S19.
29. Sakai D, Schol J, Bach FC, et al. Successful fishing for nucleus pulposus progenitor cells of the intervertebral disc across species. *JOR Spine.* 2018;1:e1018.
30. Sakai D, Nakamura Y, Nakai T, et al. Exhaustion of nucleus pulposus progenitor cells with ageing and degeneration of the intervertebral disc. *Nat Commun.* 2012;3:1264.
31. Brown S, Matta A, Erwin M, et al. Cell clusters are indicative of stem cell activity in the degenerate intervertebral disc: can their properties be manipulated to improve intrinsic repair of the disc? *Stem Cells Dev.* 2018;27:147-165.
32. Wang JY, Baer AE, Kraus VB, et al. Intervertebral disc cells exhibit differences in gene expression in alginate and monolayer culture. *Spine.* 2001;26:1747-1751.
33. Tsai TT, Guttapalli A, Oguz E, et al. Fibroblast growth factor-2 maintains the differentiation potential of nucleus pulposus cells in vitro: implications for cell-based transplantation therapy. *Spine.* 2007;32:495-502.
34. Tekari A, Chan SCW, Sakai D, Grad S, Gantenbein B. Angiopoietin-1 receptor Tie2 distinguishes multipotent differentiation capability in bovine coccygeal nucleus pulposus cells. *Stem Cell Res Ther.* 2016;7:75.
35. Sakai D, Andersson GB. Stem cell therapy for intervertebral disc regeneration: obstacles and solutions. *Nat Rev Rheumatol.* 2015;11:243-256.
36. Selard E, Shirazi-Adl A, Urban JP. Finite element study of nutrient diffusion in the human intervertebral disc. *Spine.* 2003;28:1945-1953.
37. Krouwels A, Melchels FPW, van Rijen MHP, et al. Comparing hydrogels for human nucleus pulposus regeneration: role of osmolarity during expansion. *Tissue Eng Part C Methods.* 2018;24:222-232.
38. Bergknut N, Rutges JP, Kranenburg HJ, et al. The dog as an animal model for intervertebral disc degeneration? *Spine.* 2012;37:351-358.
39. Oehme D, Goldschlager T, Ghosh P, Rosenfeld JV, Jenkin G. Cell-based therapies used to treat lumbar degenerative disc disease: a systematic review of animal studies and human clinical trials. *Stem Cells Int.* 2015;2015:946031.
40. Yang SH, Hu MH, Sun YH, Lin FH. Differential phenotypic behaviors of human degenerative nucleus pulposus cells under normoxic and hypoxic conditions: influence of oxygen concentration during isolation, expansion, and cultivation. *Spine J.* 2013;13:1590-1596.
41. Tellegen AR, Willems N, Beukers M, et al. Intradiscal application of a PCLA-PEG-PCLA hydrogel loaded with celecoxib for the treatment of back pain in canines: what's in it for humans? *J Tissue Eng Regen Med.* 2018;12:642-652.
42. Bach FC, Poramba-Liyanage DW, Riemers FM, et al. Notochordal cell-based treatment strategies and their potential in intervertebral disc regeneration. *Frontiers in Cell and Developmental Biology.* 2022;9:780749.
43. Spillekom S, Smolders LA, Grinwis GC, et al. Increased osmolarity and cell clustering preserve canine notochordal cell phenotype in culture. *Tissue Eng Part C Methods.* 2014;20:652-662.
44. Maldonado BA, Oegema TR Jr. Initial characterization of the metabolism of intervertebral disc cells encapsulated in microspheres. *J Orthop Res.* 1992;10:677-690.
45. Bach FC, de Vries SA, Krouwels A, et al. The species-specific regenerative effects of notochordal cell-conditioned medium on chondrocyte-like cells derived from degenerated human intervertebral discs. *Eur Cell Mater.* 2015;30:132-146.
46. Zuker M. Mfold web server for nucleic acid folding and hybridization prediction. *Nucleic Acids Res.* 2003;31:3406-3415.
47. Altschul SF, Madden TL, Schaffer AA, et al. Gapped BLAST and PSI-BLAST: a new generation of protein database search programs. *Nucleic Acids Res.* 1997;25:3389-3402.
48. Pfaffl MW. A new mathematical model for relative quantification in real-time RT-PCR. *Nucleic Acids Res.* 2001;29:e45.
49. Richardson SM, Ludwinski FE, Gnanalingham KK, Atkinson RA, Freemont AJ, Hoyland JA. Notochordal and nucleus pulposus marker expression is maintained by sub-populations of adult human nucleus pulposus cells through aging and degeneration. *Sci Rep.* 2017;7:1501.
50. Vogel C, Marcotte EM. Insights into the regulation of protein abundance from proteomic and transcriptomic analyses. *Nat Rev Genet.* 2012;13:227-232.
51. Rodrigues-Pinto R, Berry A, Piper-Hanley K, Hanley N, Richardson SM, Hoyland JA. Spatiotemporal analysis of putative notochordal cell markers reveals CD24 and keratins 8, 18, and 19 as notochord-specific markers during early human intervertebral disc development. *J Orthop Res.* 2016;34:1327-1340.
52. Risbud MV, Schoepflin ZR, Mwale F, et al. Defining the phenotype of young healthy nucleus pulposus cells: recommendations of the Spine Research Interest Group at the 2014 Annual ORS Meeting. *J Orthop Res.* 2015;33:283-293.

53. Peroglio M, Grad S, Mortisen D, et al. Injectable thermoreversible hyaluronan-based hydrogels for nucleus pulposus cell encapsulation. *Eur Spine J*. 2012;21(suppl 6):S839-S849.
54. Salzer E, Mouser VHM, Tryfonidou MA, Ito K. A bovine nucleus pulposus explant culture model. *J Orthop Res*. 2021. Epub ahead of print.
55. Li P, Xu Y, Gan Y, et al. Estrogen enhances matrix synthesis in nucleus pulposus cell through the estrogen receptor beta-p38 MAPK pathway. *Cell Physiol Biochem*. 2016;39:2216-2226.
56. Mavrogonatou E, Kletsas D. High osmolality activates the G1 and G2 cell cycle checkpoints and affects the DNA integrity of nucleus pulposus intervertebral disc cells triggering an enhanced DNA repair response. *DNA Repair*. 2009;8:930-943.
57. Johnson WE, Eisenstein SM, Roberts S. Cell cluster formation in degenerate lumbar intervertebral discs is associated with increased disc cell proliferation. *Connect Tissue Res*. 2001;42:197-207.
58. Xu J, Li H, Yang K, et al. Hyper-osmolality environment-induced oxidative stress injury promotes nucleus pulposus cell senescence in vitro. *Biosci Rep*. 2019;39:BSR20191711.
59. Tsai CC, Chen YJ, Yew TL, et al. Hypoxia inhibits senescence and maintains mesenchymal stem cell properties through down-regulation of E2A-p21 by HIF-TWIST. *Blood*. 2011;117:459-469.
60. van der Windt AE, Haak E, Das RH, et al. Physiological tonicity improves human chondrogenic marker expression through nuclear factor of activated T-cells 5 in vitro. *Arthritis Res Ther*. 2010;12:R100.
61. Ko BC, Turck CW, Lee KW, et al. Purification, identification, and characterization of an osmotic response element binding protein. *Biochem Biophys Res Commun*. 2000;270:52-61.
62. Cai Q, Ferraris JD, Burg MB. High NaCl increases TonEBP/OREBP mRNA and protein by stabilizing its mRNA. *Am J Physiol Renal Physiol*. 2005;289:F803-F807.
63. Woo SK, Dahl SC, Handler JS, Kwon HM. Bidirectional regulation of tonicity-responsive enhancer binding protein in response to changes in tonicity. *Am J Physiol Renal Physiol*. 2000;278:F1006-F1012.
64. Krouwels A, Popov-Celeketic J, Plomp SGM, et al. No effects of hyperosmolar culture medium on tissue regeneration by human degenerated nucleus pulposus cells despite upregulation extracellular matrix genes. *Spine*. 2018;43:307-315.
65. Gajghate S, Hiyama A, Shah M, et al. Osmolarity and intracellular calcium regulate aquaporin2 expression through TonEBP in nucleus pulposus cells of the intervertebral disc. *J Bone Miner Res*. 2009;24:992-1001.
66. Snuggs JW, Bunning RA, Le Maitre CL. Osmotic adaptation of nucleus pulposus cells: the role of aquaporin 1, aquaporin 4 and transient receptor potential vanilloid 4. *Eur Cell Mater*. 2021;41:121-141.

### SUPPORTING INFORMATION

Additional supporting information can be found online in the Supporting Information section at the end of this article.

**How to cite this article:** Laagland, L. T., Bach, F. C., Creemers, L. B., Le Maitre, C. L., Poramba-Liyanage, D. W., & Tryfonidou, M. A. (2022). Hyperosmolar expansion medium improves nucleus pulposus cell phenotype. *JOR Spine*, 5(3), e1219. <https://doi.org/10.1002/jsp2.1219>